Journal of Inorganic and General Chemistry
ZAAC
Zeitschrift für anorganische und allgemeine Chemie
DOI: 10.1002/zaac.201900313
ARTICLE

Catalytic Dehydrogenation of Amine-Boranes using Geminal Phosphino-Boranes

Devin H. A. Boom,[a] Ewoud J. J. de Boed,[a] Emmanuel Nicolas,[a] Martin Nieger,[b] Andreas W. Ehlers,[a,c] Andrew R. Jupp,[a] and J. Chris Slootweg*[a]

Dedicated to Professor Manfred Scheer on the Occasion of his 65th Birthday

Abstract. The reaction of the intramolecular frustrated Lewis pair (FLP) tBu$_2$PCH$_2$BPh$_2$ with the amine-boranes NH$_3$·BH$_3$ and Me$_2$NH·BH$_3$ leads to the formation of the corresponding FLP-H$_2$ adducts as well as novel five-membered heterocycles that result from capturing the in situ formed amino-borane by a second equivalent of FLP. The sterically more demanding tBu$_2$PCH$_2$BMes$_2$ does not form such a five-membered heterocycle when reacted with Me$_2$NH·BH$_3$ and its H$_2$ adduct liberates dihydrogen at elevated temperatures, promoting the metal-free catalytic dehydrogenation of amine-boranes.

Introduction

During the past decades tremendous breakthroughs were made in main-group mediated chemical transformations and new strategies for single bond activations were discovered. The notion that frustrated Lewis pairs (FLPs) can heterolytically cleave dihydrogen[1] spawned a new research field for metal-free stoichiometric and catalytic chemical transformations, such as hydrogenation and dehydrogenation reactions.[2]

As a substrate for catalytic dehydrogenation, amine-boranes gained a lot of attention due to their potential application as dihydrogen storage material;[3] in particular ammonia-borane (AB) is of interest as is contains a high weight percentage of dihydrogen (19.6 %).[4] Furthermore, the products resulting of amine-borane dehydrogenation are valuable, with many potential applications in materials science.[5] To date, a lot of research has been conducted on the catalytic dehydrogenation of amine-boranes by transition metal (TM) complexes.[6] Alternatively, efforts have been made in the development of group 1 and 2 catalysts,[7] and recently frustrated Lewis pairs have been reported as efficient TM-free catalysts for amine-borane dehydrogenation.[8]

The first FLP catalyst for ammonia-borane dehydrogenation was reported by *Stephan* and *Erker* (**I**, Figure 1) utilizing a transfer hydrogenation step for catalyst regeneration.[9] After this, *Uhl* and co-workers and some of us reported on the catalytic dehydrogenation of dimethylamine-borane (DMAB) by phosphino-alane **II**.[10] In 2016, *Rivard* and co-workers extended the field and showed that iminoborane **IV** can dehydrogenate methylamine-borane (MAB) at 70 °C, utilizing 2 mol-% of **IV**.[11] In the same year, *Aldridge* et al. reported that the xanthene-based phosphino-borane **V** is capable of dehydrogenating AB, MAB and DMAB with catalysts loadings down to 1 mol-%.[12] Recently *Uhl* and co-workers found that the gallium analogue of **II**, phosphino-galane **III**, can be applied for ammonia- and dimethylamine-borane dehydrogenation too.[13] At the same time, the group of *Bourissou* showed that phosphino-borane **VI** rapidly converts a variety of amine-borane substrates to the corresponding dehydrogenated products.[14]

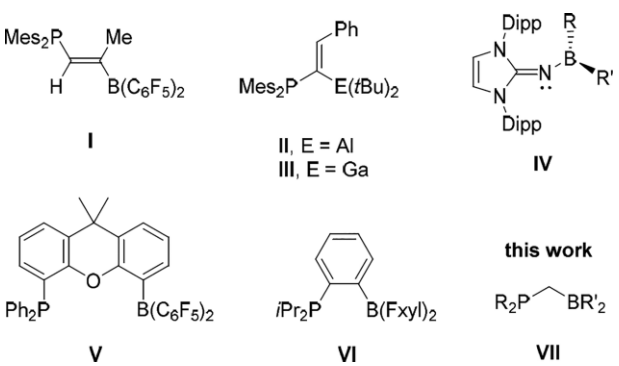

Figure 1. FLP catalysts for amine-borane dehydrogenation.

* Assoc. Prof. Dr. J. C. Slootweg
E-Mail: j.c.slootweg@uva.nl
[a] Van 't Hoff Institute for Molecular Sciences (HIMS)
University of Amsterdam
P.O. Box 94157
1090 GD Amsterdam, The Netherlands
[b] Department of Chemistry
University of Helsinki
A. I. Virtasen aukio 1
PO Box 55
00014 Helsinki, Finland
[c] Department of Chemistry, Science Faculty
University of Johannesburg
PO Box 254
Auckland Park, Johannesburg, South Africa
Supporting information for this article is available on the WWW under **http://dx.doi.org/10.1002/zaac.201900313** or from the author.

We developed geminal phosphino-borane FLP **VII** (R = *t*Bu, R′ = Ph; **1**) bearing a methylene linker, which shows reactivity towards a variety of small molecules and metal complexes.[15,16] Herein, we describe the (catalytic) dehydrogenation of amine-boranes by such geminal frustrated Lewis pairs using a rational catalyst design approach targeting increased reactivity.

Results and Discussion

Treatment of two equivalents of $tBu_2PCH_2BPh_2$ (**1**) with one equivalent of ammonia-borane ($H_3N{\cdot}BH_3$, AB) in THF at room temperature resulted in immediate consumption of AB, along with formation of dihydrogen adduct **2** ($\delta^{31}P\{^1H\}$ = 59.0 ppm) and five-membered heterocycle **3** ($\delta^{31}P\{^1H\}$ = 56.7 ppm) in a 1:1 ratio (Scheme 1). The products can be separated by extraction of **3** into *n*-pentane (leaving pure **2** as residue in 57 % yield) and subsequent filtration of the combined extracts over alumina to remove trace amounts of **2** from the extract, giving **3** as colorless solid in 74 % yield. H_2 adduct **2** displays a doublet in the ^{31}P NMR spectrum with a $^1J_{P,H}$ coupling of 453.2 Hz, and a doublet in the ^{11}B NMR spectrum ($^1J_{B,H}$ = 83.5 Hz), which is characteristic for a P–H and B–H bond, respectively. Single crystals suitable for X-ray diffraction analysis of **2** were obtained from *n*-pentane at 4 °C, which confirmed the formation of the FLP-H_2 adduct that was previously obtained from the reaction of **1** with dihydrogen.[15a] In the solid state, the boron center in **2** is strongly pyramidalized [Σ(CB1C) 330.5°], which also resembles the upfield ^{11}B NMR shift ($\delta^{11}B\{^1H\}$ = –10.1 ppm). In contrast to the *o*-phenylene-bridged P/B FLP-H_2 adduct reported by *Bourissou* and coworkers,[14] dihydrogen adduct **2** is stable at room temperature in the solid state and in solution, and only slowly released dihydrogen at elevated temperatures (2 h at 80 °C).

The formation of the five-membered heterocycle **3** is believed to be the result of trapping of the highly polarized amino-borane intermediate $H_2N{=}BH_2$ by the second equivalent of FLP **1**. In the $^{11}B\{^1H\}$ NMR spectrum, **3** displays a singlet resonance (δ = –1.95 *ppm*) for the FLP's boron moiety together with a characteristic doublet (δ = –20.7 ppm, $^1J_{B,P}$ = 85.5 Hz) that can be ascribed to the amino-borane fragment. The corresponding $^{31}P\{^1H\}$ NMR spectrum supports this notion as a broad signal was observed at δ = 56.7 ppm, which is common for such B–P interactions.[17] X-ray diffraction analysis of suitable single crystals of **3**, obtained by layering a solution of **3** in DCM with pentane, unambiguously established the formation of the P–C–B–N–B based five-membered heterocycle (Scheme 1, bottom right). Compared to the previously reported Al- and Ga-based five-membered heterocycles formed by $H_2N{=}BH_2$ trapping using the corresponding FLPs,[10,13] **3** contains a shorter P1–B2 bond [1.9606(11) Å; cf. 1.9984(14) and 2.004(2) Å, respectively], suggesting that the trapped $H_2N{=}BH_2$ fragment is more tightly bound to the FLP in **3**.

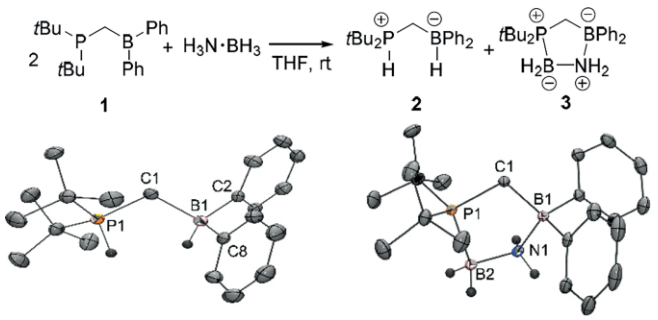

Scheme 1. Reaction of 2 equivalents of FLP **1** with 1 equivalent of ammonia-borane (top) and the molecular structures (bottom) of **2** (left) and **3** (right) (ellipsoids at 50 % probability, FLP-hydrogens, and a toluene molecule for **2** are omitted for clarity). Selected bond lengths / Å and angles /° for **2**: P1–C1 1.7759(16), B1–C1 1.683(2), P1–C1–B1 113.48(11), Σ(CB1C) 330.5 **3**: P1–C1 1.8155(10), C1–B1 1.6626(14), B1–N1 1.6321(13), N1–B2 1.5898(14), B2–P1 1.9606(11).

In order to gain more insight into the mechanism of this dehydrogenation reaction, FLP **1** was reacted with the deuterated analogue of AB, $H_3N{\cdot}BD_3$, which resulted in selective N–H to P and B–D to B transfer according to ^{31}P and ^{11}B NMR spectroscopy. This suggests a similar double hydrogen transfer mechanism being operative as was observed previously by Manners et al. for dihydrogen transfer from ammonia-borane to sterically encumbered amino-boranes.[18] Analysis of the formation of **2** by density functional theory (DFT) calculations at the ωB97X–D/6-311G** level of theory revealed that the interaction of ammonia-borane with FLP **1** leads to the formation of a three-center-two-electron adduct **4** as intermediate (Figure 2), which enables dihydrogen transfer from $H_3N{\cdot}BH_3$ in a concerted manner via a seven-membered transition state, forming phosphonium-borate **2** and one equivalent of amino-borane $H_2N{=}BH_2$. The overall process is exergonic, and the low barrier ($\Delta G^{\ddagger}$ = 13.1 kcal·mol^{-1}, $\Delta E^{\ddagger}$ = 14.3 kcal·mol^{-1}) for TS_{4-2} is in good agreement with the experimentally observed facile reaction (instantaneous at 0 °C). Additionally, trapping of the amino-borane $H_2N{=}BH_2$ fragment by a second equiva-

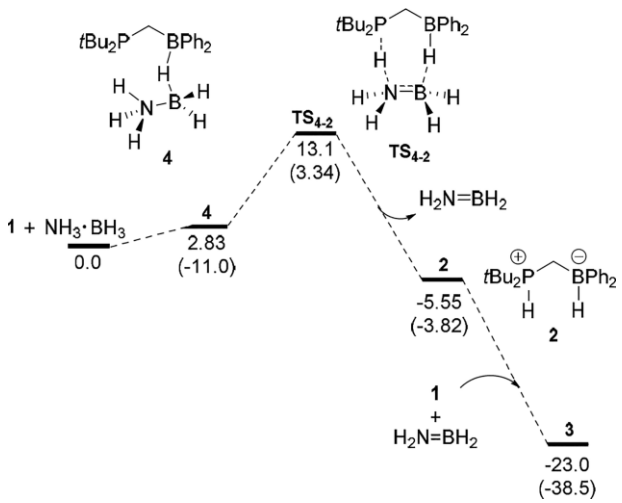

Figure 2. Gibbs free energy (and electronic energy) profile calculated for dehydrogenation of ammonia-borane by FLP **1** in kcal·mol^{-1}.

lent of FLP **1** makes the overall reaction even more exergonic ($\Delta G_{trapping}$ = –17.5 kcal·mol^{-1}, $\Delta E_{trapping}$ = –34.7 kcal·mol^{-1}).

Under the same conditions, the reaction of two equivalents of **1** with the bulkier dimethylamine-borane ($Me_2NH{\cdot}BH_3$, DMAB) resulted in rapid formation of the known FLP-H_2 adduct **2** together with the methylated analogue of **3**, compound **5** (Scheme 2). $^{31}P\{^1H\}$ NMR spectroscopy of the reaction mixture revealed comparable resonance signals as for the reaction of **1** with AB ($\delta^{31}P\{^1H\}$ = 59.0 ppm for the FLP-H_2 adduct, and a broad resonance for the methylated heterocycle; $\delta^{31}P\{^1H\}$ = 43.0 ppm). In contrast to **3**, the $^1J_{B,P}$ coupling in **5** is significantly smaller and no clear doublet was observed in the $^{11}B\{^1H\}$ NMR spectrum. DFT calculations at the ωB97X–D/6-311G** level of theory suggest that the same mechanism takes place. With an overall barrier (ΔG) of only 14.1 kcal·mol^{-1} ($\Delta E^{\ddagger}$ = 14.5 kcal·mol^{-1}), the experimentally observed reaction rate is in good agreement with the DFT calculations (see Supporting Information). Interestingly, when a sample of the reaction mixture was kept for a prolonged period at room temperature signals of the dimeric $(Me_2NBH_2)_2$ started to appear in the $^{11}B\{^1H\}$ NMR spectrum due to release of the $Me_2N{=}BH_2$ fragment from **5** and subsequent dimerization. This indicates that increasing the steric bulk of the substrate reduces the bond strength of the amino-borane fragment to FLP **1**, which suggests that increasing the steric bulk of the FLP's substituents should also prevent adduct formation.

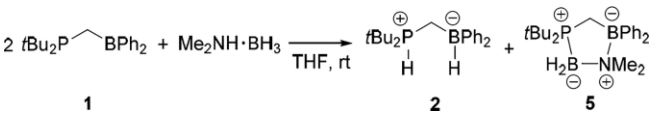

Scheme 2. Reaction of 2 equivalents of FLP **1** with dimethylamine-borane.

Encouraged by these findings, we set out to design a FLP system that disfavors amino-borane adduct formation. DFT calculations at the ωB97X–D/6-311G** level of theory showed that only a slight change of the system could already prevent adduct formation. FLP tBu$_2$PCH$_2$BMes$_2$ (**6**) bearing the bulkier mesityl substituents on boron was found to disfavor adduct formation with $Me_2N{=}BH_2$ (ΔG = 15.8 kcal·mol^{-1}), which makes **6** an interesting synthetic target for catalytic dehydrogenation. Following the same synthetic strategy used for our previously reported FLP **1**,[15a] the reaction of tBu$_2$PCH$_2$Li with one equivalent of ClBMes$_2$ cleanly afforded **6** that after work up was isolated as an orange solid in 99% yield. The $^{31}P\{^1H\}$ and $^{11}B\{^1H\}$ NMR resonances of **6** are rather similar compared to **1**, namely a sharp singlet at δ = 26.9 ppm and a broad singlet at δ = 82.5 ppm, respectively. X-ray diffraction analysis of orange crystals obtained by cooling a saturated heptane solution of **6** to –20 °C showed that the boron empty p-orbital is rotated away from the phosphorus lone-pair (torsion angle P1–C1–B1–C11 = 168.9°) and that the boron center bears a planar arrangement [$\sum$(CB1C) = 359.8°], making any LA···LB type of interaction negligible in the solid state (Scheme 3). The physical appearance of FLP **6** is noteworthy; whereas phenyl-substituted FLP **1** is an oil at room temperature, the mesityl-substituted analogue **6** is a solid, which facilitates the handling of the compound.

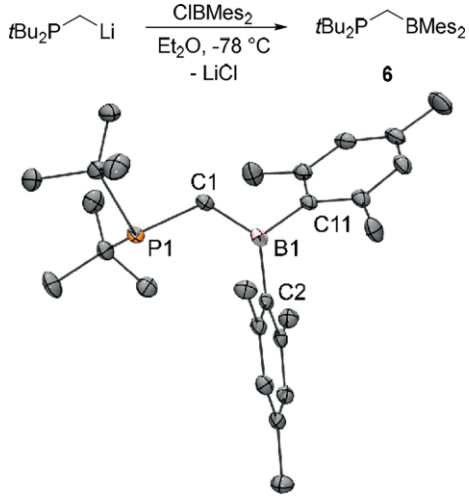

Scheme 3. Synthesis of FLP **6** (top) and its molecular structure (bottom; ellipsoids at 50% probability, hydrogen atoms are omitted for clarity). Selected bond lengths /Å and angles /° for **6**: P1–C1 1.8605(17), C1–B1 1.582(3), P1–C1–B1 124.21(12), P1–C1–B1–C11 168.94(12), Σ(CB1C) 359.8.

Under similar conditions, FLP **6** (two equivalents) was reacted with one equivalent of ammonia-borane in 2-MeTHF (2-methyltetrahydrofuran) at room temperature. After approximately 1 h at room temperature, the $^{11}B\{^1H\}$ and $^{31}P\{^1H\}$ NMR spectra of the reaction mixture revealed that **6** was fully converted into FLP-H_2 adduct **7** [$\delta^{31}P\{^1H\}$ = 56.5 (s); $^{11}B\{^1H\}$ = –15.0 (s)] and the five-membered heterocycle **8** [$\delta^{31}P\{^1H\}$ = 58.1 (br. s); $^{11}B\{^1H\}$ = 1.95 (s), –23.2 (s)], along with the formation of traces of dehydrogenation products such as borazine, cyclotriborazane (CTB) and *B*-(cyclodiborazanyl)aminoborohydride (BCDB) and a few unidentified products (Scheme 4).

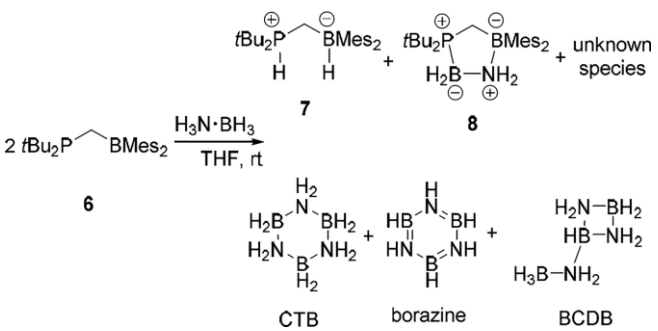

Scheme 4. The reaction of 2 equivalents of **6** with dimethylamine-borane.

Interestingly, heating the reaction mixture to 70 °C led to almost complete disappearance of H_2 adduct **7** and heterocycle **8**, concomitant with an increase of dehydrogenation products together with the formation of degradation products, such as $Mes_2B{=}NH_2$ [$\delta^{11}B\{^1H\}$ = 44.1 (br. s)][19] and tBu$_2$PCH$_3{\cdot}$BH$_3$ [$\delta^{31}P\{^1H\}$ = 39.9 (m); $^{11}B\{^1H\}$ = –40.8 (d, $^1J_{B,P}$ = 57.8 Hz)], as was observed by $^{11}B\{^1H\}$ and $^{31}P\{^1H\}$ NMR spectroscopy.

In addition, regeneration of FLP **6** was observed, suggesting that **6** could play a role in catalytic amine-borane dehydrogenation, which is significant as only a few FLPs are reported to catalyze the dehydrogenation of AB.[12–14]

The labile character of both the FLP-H_2 adduct **7** and the five-membered heterocycle **8** inspired us to investigate the possibility to apply **6** as a catalyst for ammonia-borane dehydrogenation. When 4 mol-% of **6** was added to a suspension of $H_3N{\cdot}BH_3$ in 2-MeTHF, **6** was directly converted to H_2 adduct **7** and heterocycle **8** according to $^{11}B\{^1H\}$ and $^{31}P\{^1H\}$ NMR spectroscopy. When the reaction mixture was heated to 70 °C, a modest evolution of dihydrogen gas was visually observed as bubbles appeared from the reaction mixture. After 20 minutes at 70 °C, a mixture of dehydrogenation products was formed, yet the H_2 adduct **7** was still observable in both the $^{11}B\{^1H\}$ and $^{31}P\{^1H\}$ NMR spectrum, suggesting that this H_2 adduct is the resting state of the catalytic cycle. Prolonging the reaction time to 2 h at 70 °C resulted in an increase of dehydrogenation B–N products and full degradation of the catalyst to $t\mathrm{Bu_2PCH_3{\cdot}BH_3}$ and $\mathrm{Mes_2B{=}NH_2}$, and neither free FLP **6** nor the dihydrogen adduct **7** were observed by NMR spectroscopy.

DFT calculations at the ωB97X–D/6-311G** level of theory confirm that dihydrogen adduct **7** is a plausible resting state in the catalytic dehydrogenation of AB. Similar to **1**, the calculations suggest that the initial interaction via a three-center-two-electron adduct is followed by a concerted double hydrogen abstraction step ($\Delta G^{\ddagger}$ = 25.1 kcal·mol^{-1}, $\Delta E^{\ddagger}$ = 16.3 kcal·mol^{-1}; Figure 3). This reaction step forming H_2 adduct **7** and $H_2N{=}BH_2$ was found to be exergonic by 6.13 kcal·mol^{-1} (ΔG) and 4.70 kcal·mol^{-1} (ΔE). The energy barrier for dihydrogen release from **7** is the rate-determining step ($\Delta G^{\ddagger}$ = 27.3 kcal·mol^{-1}, $\Delta E^{\ddagger}$ = 28.6 kcal·mol^{-1}), which explains why H_2 adduct **7** can be observed by NMR spectroscopy during the reaction and why release of dihydrogen is observed after the reaction mixture is heated to elevated temperatures.

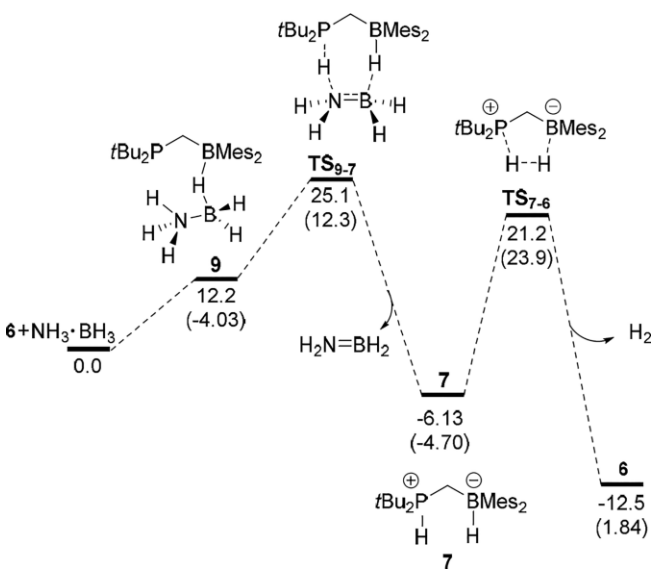

Figure 3. Gibbs free energy (and electronic energy) profile calculated for AB dehydrogenation by **6** in kcal·mol^{-1}.

Under our standard catalytic conditions (4 mol-% of **6**, 70 °C, 2.1 M DMAB, in 2-MeTHF) dimethylamine-borane was set for dehydrogenation (Scheme 5). Initial formation of the FLP-H_2 adduct **7** was observed by $^{31}P\{^1H\}$ NMR spectroscopy, while upon heating to 70 °C this species disappeared and the formation of dimeric $(Me_2NBH_2)_2$ was observed in the ^{11}B NMR spectrum, along with traces of other dehydrogenation products as well as the evolution of dihydrogen gas. Prolonging the reaction time resulted in an increase of $(Me_2NBH_2)_2$ formation which was monitored by ^{11}B NMR spectroscopy utilizing a sealed capillary filled with $B(OMe)_3$ as internal standard. Over time, FLP **6** continuously consumed the $Me_2NH{\cdot}BH_3$ substrate, while producing the amino-borane dimer. Concomitant to the catalytic dehydrogenation, slow decomposition of the FLP catalyst **6** to $t\mathrm{Bu_2PCH_3{\cdot}BH_3}$ and several other unknown degradation products was observed. Eventually after 6 days at 70 °C, **6** was completely degraded and the production of $(Me_2NBH_2)_2$ stopped. Important to note is that in the absence of FLP **6**, no dehydrogenation was observed under the same reaction conditions.

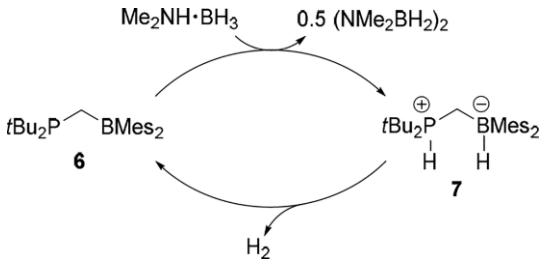

Scheme 5. Catalytic dehydrogenation of dimethylamine-borane by FLP **6**.

The highest turnover number (TON) was obtained with 4 mol-% catalyst loading at 70 °C, reaching 23 turnovers after 6 days. For comparison, a range of Ru pincer complexes performed the same reaction with TONs of between 2 and 99 after 24 h.[20] The turnover frequency (TOF) after approximately 10% conversion of the dimethylamine-borane substrate at 50 °C was found to be 0.62 h^{-1}, which is not high, but is comparable with several transition metal complexes reported by *Travieso-Puente* and co-workers.[21] As expected, higher TOFs were obtained at higher temperatures and after approximately 10% conversion at 60, 70, and 80 °C TOFs of 1.89, 2.65, and 4.36 h^{-1} were obtained, respectively. At these elevated temperatures faster catalyst decomposition was observed resulting in lower turnover frequencies as the conversion increases.

Since a minor modification of our original FLP $t\mathrm{Bu_2PCH_2BPh_2}$ (**1**) affords $t\mathrm{Bu_2PCH_2BMes_2}$ (**6**) that changed the reactivity towards dimethylamine-borane from stoichiometric to catalytic dehydrogenation, we envision that additional changes of the P- and B-substituents might further increase the activity of the FLP catalyst, which is an ongoing endeavor in our laboratories.

Conclusions

$t\mathrm{Bu_2PCH_2BPh_2}$ (**1**) conveniently dehydrogenates ammonia-borane and dimethylamine-borane to form the FLP-H_2 adduct

2 and a new five-membered heterocycle **3**. DFT calculations revealed that the underlying mechanism operates via formation of a three-center-two-electron adduct, which is followed by a concerted double hydrogen abstraction step involving a seven-membered transition state. The bulkier tBu$_2$PCH$_2$BMes$_2$ (**6**) was designed and subsequently synthesized in excellent yields, and shows catalytic activity towards ammonia-borane and dimethylamine-borane.

Experimental Section

Materials and Methods: All manipulations were carried out in an atmosphere of dry nitrogen, using standard Schlenk and drybox techniques. Solvents were purified, dried and degassed according to standard procedures and stored under 3 Å molecular sieves or a sublimed sodium mirror. ^{1}H and ^{13}C{^{1}H} NMR spectra were recorded on a Bruker Avance 400 or Bruker Avance 500 and internally referenced to the residual solvent resonances ($CDCl_3$: ^{1}H δ = 7.26, ^{13}C{^{1}H} δ = 77.2; [D$_8$]THF: ^{1}H δ = 3.58, 1.72, ^{13}C{^{1}H} δ = 67.2, 25.3; C_6D_6: ^{1}H δ = 7.16, ^{13}C{^{1}H} 128.1; Tol-d_8: ^{1}H δ = 7.09, 7.01, 6.97, 2.08, ^{13}C{^{1}H} δ = 137.48, 128.87, 127.96, 125.13, 20.43). ^{31}P{^{1}H}, ^{31}P, ^{11}B{^{1}H} and ^{11}B NMR spectra were recorded on a Bruker Avance 400 and externally referenced (85 % H_3PO_4, BF_3·OEt_2, respectively). High resolution mass spectra were recorded on a Bruker MicroTOF with ESI nebulizer (ESI). Melting points were measured in sealed capillaries and are uncorrected. tBu$_2$PCH$_2$Li,[22] and tBu$_2$PCH$_2$BPh$_2$ (**1**)[15a] were synthesized following literature procedures. 2-MeTHF was purchased from Sigma Aldrich and subsequently degassed and dried with 3 Å molecular sieves. NH_3·BH_3, $NHMe_2$·BH_3, PBr_3, MesMgBr (1 M in THF), $LiAlH_4$, nBuLi (1.6 M in hexane), tBuLi (1.7 M in pentane), MeLi (1.6 M in Et_2O), BCl_3 (1 M in heptane) and $B(OMe)_3$ were purchased from Sigma Aldrich, and all were used without any further purification.

Preparation of tBu$_2$PCH$_2$BPh$_2$–H$_2$ Adduct 2:[15a] A THF stock solution of ammonia-borane (28.84 mL, 0.1 M, 2.88 mmol, 1.0 equiv.) was added to a solution of tBu$_2$PCH$_2$BPh$_2$ (**1**, 1.87 gr, 5.77 mmol, 2.0 equiv.) in THF (15 mL) at 0 °C. After addition, the reaction mixture was warmed to room temperature and all volatiles were removed in vacuo. The obtained colorless solid was thoroughly washed with n-pentane (3 × 20 mL) and the solids were subsequently dried in vacuo to afford **2** as a colorless solid (0.536 g, 57 %). Colorless X-ray quality crystals were obtained from a solution of **2** in n-pentane which was stored at 4 °C. **^{1}H NMR** (400.13 MHz, [D$_8$]THF, 293 K): δ = 7.32 (d, $^3J_{H,H}$ = 7.1 Hz, 4 H, o-PhH), 6.97 (t, $^3J_{H,H}$ = 7.4 Hz, 4 H, m-PhH), 6.82 (t, $^3J_{H,H}$ = 7.3 Hz, 2 H, p-PhH), 4.96 (dt, $^1J_{H,P}$ = 453.2, $^3J_{H,H}$ = 4.8 Hz, 1 H, PH), 3.12–2.29 (br. m, 1 H, BH), 1.26 [d, $^3J_{H,P}$ = 14.8 Hz, 18 H, C(CH_3)$_3$], 1.19–1.10 (br. m, 2 H, PCH_2B). **^{31}P{^{1}H} NMR** (162.0 MHz, [D$_8$]THF, 293 K): δ = –10.1 (s). **^{11}B{^{1}H} NMR** (128.4 MHz, [D$_8$]THF, 293 K): δ = 59.0 (s) ppm.

Preparation of tBu$_2$PCH$_2$BPh$_2$–NH$_2$BH$_2$ Adduct 3: A THF stock solution of ammonia-borane (28.84 mL, 0.1 M, 2.88 mmol, 1.0 equiv.) was added to a solution of tBu$_2$PCH$_2$BPh$_2$ (**1**, 1.87 gr, 5.77 mmol, 2.0 equiv.) in THF (15 mL) at 0 °C. After addition, the reaction mixture was warmed to room temperature and all volatiles were removed in vacuo. The obtained white solid was thoroughly extracted in n-pentane (3 × 20 mL). The combined extracts were filtered through a pad of alumina, which was subsequently flushed with 250 mL eluent (cyclohexane/ethyl acetate 20:1, resp.). The collected filtrate was dried in vacuo to afford **3** as a colorless solid (0.754 g, 74 %). X-ray quality crystals were obtained from a solution of **3** (289 mg) in a pentane/DCM mixture (7.5 mL : 0.54 mL) which was stored at 4 °C. Mp. (nitrogen, sealed capillary): 128 °C. **^{1}H NMR** (400.13 MHz, [D$_8$]THF, 293 K): δ = 7.29 (d, $^3J_{H,H}$ = 7.1 Hz, 4 H, o-PhH), 7.03, (t, $^3J_{H,H}$ = 7.4 Hz, 4 H, m-PhH), 6.89 (t, $^3J_{H,H}$ = 7.2 Hz, 2 H, p-PhH), 3.37 (br. s, 2 H, NH_2), 2.80–1.75 (br. m, 2 H, BH_2), 1.19–1.13 (m, 20 H, PCH_2B, C(CH_3)$_3$). **^{13}C{^{1}H} NMR** (100.62 MHz, [D$_8$]THF, 293 K): δ = 157.0 (br. s; $ipso$-PhC), 132.1 (s; o-PhC), 127.2 (s; m-PhC), 124.4 (s; p-PhC), 31.8 (d; $^1J_{C,P}$ = 25.8 Hz; C(CH$_3$)$_3$), 28.1 (d; $^2J_{C,P}$ = 1.2 Hz; C(CH_3)$_3$), 9.0 (s; PCH_2B). **^{31}P{^{1}H} NMR** (162.0 MHz, [D$_8$]THF, 293 K): δ = 56.7 (br. m). **^{11}B{^{1}H} NMR** (128.4 MHz, [D$_8$]THF, 293 K): δ = –1.95 ppm(s; BPh$_2$), –20.7 (d, $^1J_{B,P}$ = 85.5 Hz; PBH$_2$N) ppm. **HR-MS (ESI)**: 352.2554 [**3**–H]$^+$, calcd. for: $C_{21}H_{33}B_2NP^+$ 352.25312.

Preparation of Mes$_2$BOMe:[23] A solution of MesMgBr (1 M in THF, 27 mL, 27 mmol, 2.1 equiv.) was added dropwise to a solution of $B(OMe)_3$ (1.45 mL, 1.35 g, 13 mmol, 1.0 equiv.) in THF (15 mL), which resulted in a grey suspension that turned into a brown solution after heating to 55 °C for 5h and subsequent stirring at room temperature overnight. The volatiles were removed in vacuo and the mixture was extracted into n-pentane (40 + 18 mL). The combined extracts were dried in vacuo to yield a colorless solid (2.98 g, 82 %). Crystallization of this compound was possible from a solution in hot methanol (10 mL·g^{-1} product) to afford colorless crystals upon cooling. **^{1}H NMR** (500.23 MHz, $CDCl_3$, 293 K): δ = 6.79 (s, 4 H, Mes$H$), 3.75 (s, 3 H, OCH_3), 2.27 (s, 6 H, p-MesCH_3), 2.22 (s, 12 H, o-MesCH_3). **^{13}C{^{1}H} NMR** (125.80 MHz, $CDCl_3$, 293 K): δ = 128.3 (br. s; m-Mes$C$), 54.3 (s; OCH$_3$), 22.4 (s; o-Mes$C$H$_3$), 21.3 (s; p-Mes$C$H$_3$), the signals for $ipso$-Mes$C$, o-Mes$C$ and p-Mes$C$ are unresolved. **^{11}B{^{1}H} NMR** (128.38 MHz, $CDCl_3$, 293 K): δ = 45.0 (br. s) ppm.

Preparation of Mes$_2$BCl:[24] A solution of BCl_3 (1 M in heptane, 19 mL, 19 mmol, 1.3 equiv.) was added dropwise to a solution of Mes$_2$BOMe (4.13 g, 14.8 mmol, 1.0 equiv.) in heptane (20 mL) at room temperature, after which the mixture was heated overnight at 60 °C. The reaction mixture was cooled to room temperature and the volatiles were removed in vacuo to offer pinkish solids that were extracted into n-pentane (12 + 20 mL). The combined extracts were dried in vacuo, which afforded a colorless solid (3.86 g, 92 %). X-ray quality crystals were obtained by recrystallization from hot pentane (2.6 mL·g^{-1} crude Mes$_2$BCl) and subsequent washing with pentane (0.5 mL·g^{-1} crude) at –80 °C to afford colorless crystals. Mp. (nitrogen, sealed capillary): 80–84 °C (trajectory). **^{1}H NMR** (500.23 MHz, $CDCl_3$, 293 K): δ = 6.83 (s, 4 H, Mes-H), 2.30 (s, 12 H, o-MesCH_3), 2.28 (s, 6 H, p-MesCH_3). **^{13}C{^{1}H} NMR** (125.80 MHz, $CDCl_3$, 293 K): δ = 140.9 (s; o-Mes$C$), 140.5 (s; p-Mes$C$), 129.0 (s; m-Mes$C$), 23.4 (s; o-Mes$C$H$_3$), 21.4 (s; p-MesCH$_3$), the signal for $ipso$-Mes$C$ is unresolved. **^{11}B{^{1}H} NMR** (128.38 MHz, $CDCl_3$, 293 K): δ = 69.9 (br. s) ppm.

Preparation of tBu$_2$PCH$_2$BMes$_2$ (6): A solution of Mes$_2$BCl (3.47 g, 12.2 mmol, 1.0 equiv.) in Et_2O (15 mL) was added dropwise to a suspension of tBu$_2$PCH$_2$Li (2.72 g, 16.4 mmol, 1.3 equiv.) in Et_2O (15 mL) at –80 °C and after addition the reaction mixture was warmed to room temperature. After 2.5 d of stirring at room temperature, the suspension was concentrated in vacuo which afforded an orange foam. The foam was extracted into n-pentane (25 mL) and filtered through a Schlenk filter packed with Celite. Subsequently, the Celite layer was extracted into pentane (3 × 10 mL) and the combined extracts were concentrated in vacuo, which afforded an orange solid (4.94 g, 99 %). X-ray quality crystals were obtained from a solution of 0.45 g of **6** in 1 mL of hot heptane (80–85 °C) and subsequent slow cooling to –20 °C. Mp. (nitrogen, sealed capillary): 79–87 °C (trajectory). **^{1}H NMR** (400.13 MHz, C_6D_6, 293 K): δ = 6.77 (s, 4 H, Mes$H$), 2.43 (s, 12 H, o-MesCH_3), 2.15 (s, 6 H, p-MesCH_3), 2.09 (d, $^2J_{H,P}$ = 4.7 Hz, 2 H, PCH_2B), 1.08 (d, $^2J_{H,P}$ = 10.5 Hz, 18 H, C(CH_3)$_3$). **^{13}C{^{1}H} NMR**

(100.62 MHz, C_6D_6, 293 K): δ = 143.4 (only observed in the HMBC spectrum, $^3J_{C,H}$ coupling with Mes*H*, *o*-MesCH_3, and PCH_2B; *ipso*-Mes*C*), 139.1 (s; *o*-Mes*C*), 138.3 (s; *p*-Mes*C*), 129.2 (s; *m*-Mes*C*), 31.5 [d, $^1J_{C,P}$ = 25.1 Hz; *C*$(CH_3)_3$], 30.0 [d, $^1J_{C,P}$ = 14.1 Hz; C(*C*$H_3)_3$], 28.1 (only observed in the HSQC spectrum, $^1J_{C,H}$ coupling with PCH_2B; PCH_2B), 24.1 (2 x s; *o*-Mes*C*H_3), 21.2 (s; *p*-Mes*C*H_3). **^{31}P{^{1}H} NMR** (161.97 MHz, [D_8]toluene, 293 K): δ = 26.9 (s). **^{11}B{^{1}H} NMR** (128.38 MHz, [D_8]toluene, 293 K): δ = 82.0 (br. s) ppm. **HR-MS (ESI)**: 409.3200 [6+H]$^+$, calcd. for $C_{27}H_{43}BP^+$ 409.3190.

Stability of *t*Bu$_2$PCH$_2$BPh$_2$–H$_2$ Adduct (2) towards Heating: A NMR sample containing a solution of **2** in 2-MeTHF was heated to 50 °C for 3 h, after which ^{31}P{^{1}H} spectroscopy revealed no formation of *t*Bu$_2$PCH$_2$Ph$_2$ and only 2% decomposition to *t*Bu$_2$PCH$_3$. Subsequent heating to 80 °C for 2 h resulted in liberation of dihydrogen and 17% conversion to *t*Bu$_2$PCH$_2$Ph$_2$ as well as 18% decomposition to *t*Bu$_2$PCH$_3$.

Reaction of *t*Bu$_2$PCH$_2$BMes$_2$ (6) with 0.5 Equiv. of NH$_3$BH$_3$: A screw-cap NMR tube was charged with ammonia-borane (0.0054 g, 0.175 mmol, 1.0 equiv.), *t*Bu$_2$PCH$_2$BMes$_2$ (**6**, 0.1428 g, 0.350 mmol, 2.0 equiv.) and 2-MeTHF (6 mL). The reaction mixture was kept at room temperature and analyzed after 1 h with ^{31}P{^{1}H}, ^{11}B{^{1}H} and ^{11}B NMR spectroscopy, showing a mixture of dehydrogenated ammonia-borane products [^{11}B{^{1}H} NMR: δ = 30.8 (borazine), –4.94 (BCDB), –11.2 (CTB)], along with the formation of the H_2 adduct **7** [^{11}B NMR: δ = –15.0 (d, $^1J_{B,H}$ = 81.1 Hz); ^{31}P{^{1}H} NMR: δ = 56.5 (s)] and five-membered heterocycle **8** [^{11}B NMR: δ = 1.92 (s), –23.3 (t, $^1J_{B,H}$ = 72.9 Hz); ^{31}P{^{1}H} NMR: δ = 58.1 (br. s)]. Subsequently, the reaction mixture was heated to 70 °C overnight and a white suspension was obtained (solids are postulated to be polyborazine) and ^{31}P{^{1}H}, ^{11}B and ^{11}B{^{1}H} NMR spectroscopy revealed complete consumption of the H_2 adduct **7** and heterocycle **8**, as well as an increase in formation of borazine, polyborazine [^{11}B NMR: δ = 24.8 (s)], formation of two unidentified products [^{11}B NMR: δ = –23.4 (s) and –29.8 (s)], decomposition to Mes$_2$B=NH$_2$ [^{11}B NMR: δ = 43.7 (s)] and *t*Bu$_2$PCH$_3$·BH$_3$ [^{11}B NMR: δ = –41.6 (dq, $^1J_{B,H}$ = 96.4, $^1J_{B,P}$ = 57.9 Hz; ^{31}P{^{1}H} NMR: δ = 39.9 (br. q)], and lastly also regeneration of FLP **6**.

Reaction of *t*Bu$_2$PCH$_2$BMes$_2$ (6) with 25 Equiv. of NH$_3$BH$_3$: A screw-cap NMR tube was charged with ammonia-borane (0.031 g, 1.357 mmol, 25.0 equiv.), *t*Bu$_2$PCH$_2$BMes$_2$ (**6**, 0.022 g, 0.054 mmol, 1.0 equiv.) and 2-MeTHF (6 mL). The reaction mixture was mixed at room temperature and directly analyzed by ^{31}P{^{1}H}, ^{11}B{^{1}H} and ^{11}B NMR spectroscopy, which revealed formation of the H_2 adduct **7** and the five-membered heterocycle **8**. Subsequently, the NMR tube was heated to 70 °C and analyzed by NMR spectroscopy after 20 and 120 minutes, after which complete consumption of FLP **6** and H_2 adduct **7** was observed, along with the formation of dehydrogenation products and dihydrogen gas.

X-ray Crystallography: The single-crystal X-ray diffraction studies were carried out on a Bruker-Nonius KappaCCD diffractometer at 123(2) K using Mo-K_α radiation (λ = 0.71073 Å) (**2**, **6**) or Bruker D8 Venture diffractometer with Photon100 detector at 123(2) K using Mo-K_α radiation (λ = 0.71073 Å) (**3**). Direct Methods (SHELXS-97)[25] were used for structure solution and refinement was carried out using SHELXL-2013/2014 (full-matrix least-squares on F^2).[26] Hydrogen atoms were localized by difference electron density determination and refined using a riding model (H(B, N, P) free). Semi-empirical absorption corrections were applied. For **3** an extinction correction was applied.

2: Colorless crystals, $C_{21}H_{32}BP{\cdot}0.5(C_7H_8)$, M_r = 372.31, crystal size 0.50 × 0.30 × 0.20 mm, monoclinic, space group *C*2/*c* (no.15), *a* = 32.562(4) Å, *b* = 8.776(1) Å, *c* = 17.801(2) Å, β = 118.75(1)°, *V* = 4459.8(10) Å^3, *Z* = 8, ρ = 1.109 Mg·m^{-3}, μ(Mo-K_α) = 0.13 mm^{-1}, *F*(000) = 1624, $2\theta_{max}$ = 55°, 25741 reflections, of which 5128 were independent (R_{int} = 0.039), 243 parameters, 38 restraints, R_1 = 0.049 [for 4179 $I > 2\sigma(I)$], wR_2 = 0.123 (all data), *S* = 1.03, largest diff. peak / hole = 0.88 / –0.44 e·Å^{-3}.

3: Colorless crystals, $C_{21}H_{34}B_2NP$, M_r = 353.08, crystal size 0.48 × 0.48 × 0.36 mm, triclinic, space group $P\bar{1}$ (no.2), *a* = 9.0523(5) Å, *b* = 10.2844(6) Å, *c* = 13.0205(8) Å, α = 100.971(2)°, β = 108.436(2)°, γ = 104.693(2)°, *V* = 1062.92(11) Å^3, *Z* = 2, ρ = 1.103 Mg·m^{-3}, μ(Mo-K$_\alpha$) = 0.13 mm^{-1}, *F*(000) = 384, $2\theta_{max}$ = 55°, 36356 reflections, of which 4902 were independent (R_{int} = 0.022), 239 parameters, 4 restraints, R_1 = 0.032 [for 4554 $I > 2\sigma(I)$], wR_2 = 0.085 (all data), *S* = 1.05, largest diff. peak / hole = 0.35 / –0.28 e·Å^{-3}.

6: Orange crystals, $C_{27}H_{42}BP$, M_r = 408.38, crystal size 0.60 × 0.45 × 0.40 mm, monoclinic, space group $P2_1/c$ (no.14), *a* = 12.842(1) Å, *b* = 10.033(1) Å, *c* = 20.516(2) Å, β = 104.46(1)°, *V* = 2559.6(4) Å^3, *Z* = 4, ρ = 1.060 Mg·m^{-3}, μ(Mo-K_α) = 0.12 mm^{-1}, *F*(000) = 896, $2\theta_{max}$ = 55°, 24882 reflections, of which 5871 were independent (R_{int} = 0.054), 268 parameters, R_1 = 0.050 [for 4666 $I > 2\sigma(I)$], wR_2 = 0.135 (all data), *S* = 1.04, largest diff. peak / hole = 0.40 / –0.35 e·Å^{-3}.

Crystallographic data (excluding structure factors) for the structures in this paper have been deposited with the Cambridge Crystallographic Data Centre, CCDC, 12 Union Road, Cambridge CB21EZ, UK. Copies of the data can be obtained free of charge on quoting the depository numbers CCDC-1967181 (**2**), CCDC-1967182 (**3**), and CCDC-1967183 (**6**) (Fax: +44-1223-336-033; E-Mail: deposit@ccdc.cam.ac.uk, http://www.ccdc.cam.ac.uk)

Computational Details: All structures were optimized at the ωB97X–D level of theory,[27] using Gaussian 09, Revision D01.[28] Geometry optimizations were performed using the 6-311G(d,p) basis set,[29,30] and the nature of each stationary point was confirmed by frequency calculations.

Supporting Information (see footnote on the first page of this article): Cartesian coordinates for all computed structures and a video of the catalytic dehydrogenation of DMAB with **6**.

Acknowledgements

This work was supported by the Council for Chemical Sciences of The Netherlands Organization for Scientific Research (NWO/CW) by a VIDI grant (J.C.S.) and a VENI grant (A.R.J.). J.C.S. acknowledges the Alexander von Humboldt Foundation for a Humboldt Research Fellowship for Experienced Researchers. We gratefully acknowledge *Ed Zuidinga* for mass spectrometric analyses and *Ibrahim Aydin* for obtaining suitable crystals of compound **3**.

Keywords: Frustrated Lewis pairs; Amine-boranes; Dehydrogenation; Main-group catalysis; Density functional calculations

References

[1] G. C. Welch, R. R. S. Juan, J. D. Masuda, D. W. Stephan, *Science* **2006**, *314*, 1124–1126.

[2] For an overview of developments in FLP chemistry, see: a) D. W. Stephan, G. Erker, *Angew. Chem. Int. Ed.* **2010**, *49*, 46–76; b) D. W. Stephan, *Acc. Chem. Res.* **2015**, *48*, 306–316; c) D. W. Stephan, *Science* **2016**, *354*, 1248; d) A. R. Jupp, D. W. Stephan, *Trends Chem.* **2019**, *1*, 35–48.
[3] C. W. Hamilton, R. T. Baker, A. Staubitz, I. Manners, *Chem. Soc. Rev.* **2009**, *38*, 279–293.
[4] a) T. B. Marder, *Angew. Chem. Int. Ed.* **2007**, *46*, 8116–8118; b) A. Staubitz, A. P. M. Robertson, M. E. Sloan, I. Manners, *Chem. Rev.* **2010**, *110*, 4023–4078; c) A. Staubitz, A. P. M. Robertson, I. Manners, *Chem. Rev.* **2010**, *110*, 4079–4124.
[5] E. M. Leitao, T. Jurca, I. Manners, *Nat. Chem.* **2013**, *5*, 817–829.
[6] For reviews about transition metal based amine-borane dehydrogenation catalysts, see: a) N. C. Smythe, J. C. Gordon, *Eur. J. Inorg. Chem.* **2010**, 509–521; b) N. E. Stubbs, A. P. M. Robertson, E. M. Leitao, I. Manners, *J. Organomet. Chem.* **2013**, *730*, 84–89; c) A. Rossin, M. Peruzzini, *Chem. Rev.* **2016**, *116*, 8848–8872; d) S. Bhunya, T. Malakar, G. Ganguly, A. Paul, *ACS Catal.* **2016**, *6*, 7907–7934.
[7] For reviews on group 1 and 2 metal-based amine-borane dehydrogenation catalysts, see: a) R. J. Less, R. L. Melen, D. S. Wright, *RSC Adv.* **2012**, *2*, 2191–2199; b) R. L. Melen, *Chem. Soc. Rev.* **2016**, *45*, 775–788.
[8] For a recent review, see: D. H. A. Boom, A. R. Jupp, J. C. Slootweg, *Chem. Eur. J.* **2019**, *25*, 9133–9152.
[9] a) D. W. Stephan, G. Erker, *Angew. Chem. Int. Ed.* **2010**, *49*, 46–76; b) D. W. Stephan, G. Erker, *Angew. Chem. Int. Ed.* **2015**, *54*, 6400–6441.
[10] C. Appelt, J. C. Slootweg, K. Lammertsma, W. Uhl, *Angew. Chem. Int. Ed.* **2013**, *52*, 4256–4259.
[11] M. W. Lui, N. R. Paisley, R. McDonald, M. J. Ferguson, E. Rivard, *Chem. Eur. J.* **2016**, *22*, 2134–2145.
[12] Z. Mo, A. Rit, J. Campos, E. L. Kolychev, S. Aldridge, *J. Am. Chem. Soc.* **2016**, *138*, 3306–3309.
[13] J. Possart, W. Uhl, *Organometallics* **2018**, *37*, 1314–1323.
[14] M. Boudjelel, E. D. S. Carrizo, S. Mallet-Ladeira, S. Massou, K. Miqueu, G. Bouhadir, D. Bourissou, *ACS Catal.* **2018**, *8*, 4459–4464.
[15] Reactivity towards small molecules: a) F. Bertini, V. Lyaskovskyy, B. J. J. Timmer, F. J. J. de Kanter, M. Lutz, A. W. Ehlers, J. C. Slootweg, K. Lammertsma, *J. Am. Chem. Soc.* **2012**, *134*, 201–204; b) E. R. M. Habraken, L. C. Mens, M. Nieger, M. Lutz, A. W. Ehlers, J. C. Slootweg, *Dalton Trans.* **2017**, *46*, 12284–12292; c) D. H. A. Boom, A. R. Jupp, M. Nieger, A. W. Ehlers, J. C. Slootweg, *Chem. Eur. J.* **2019**, *25*, 13299–13308.
[16] Reactivity towards transition metals: a) D. H. A. Boom, A. W. Ehlers, M. Nieger, J. C. Slootweg, *Z. Naturforsch. B* **2017**, *72*, 781–784; b) D. H. A. Boom, A. W. Ehlers, M. Nieger, M. Devillard, G. Bouhadir, D. Bourissou, J. C. Slootweg, *ACS Omega* **2018**, *3*, 3945–3951.
[17] For examples of cyclic phosphine-boranes see: H. Schmidbaur, M. Sigl, A. Schier, *J. Organomet. Chem.* **1997**, *529*, 323–327.
[18] a) A. P. M. Robertson, E. M. Leitao, I. Manners, *J. Am. Chem. Soc.* **2011**, *133*, 19322–19325; b) E. M. Leitao, N. E. Stubbs, A. P. M. Robertson, H. Helten, R. J. Cox, G. C. Lloyd-Jones, I. Manners, *J. Am. Chem. Soc.* **2012**, *134*, 16805–16816.
[19] a) N. M. D. Brown, F. Davidson, J. W. Wilson, *J. Organomet. Chem.* **1980**, *192*, 133–138; b) R. A. Bartlett, H. Chen, V. R. Dias, M. M. Olmstead, P. P. Power, *J. Am. Chem. Soc.* **1988**, *110*, 446–449.
[20] M. J. Sgro, D. W. Stephan, *Dalton Trans.* **2013**, *42*, 10460–10472.
[21] D. García-Vivó, E. Huergo, M. A. Ruiz, R. Travieso-Puente, *Eur. J. Inorg. Chem.* **2013**, 4998–5008.
[22] F. Eisenträger, A. Göthlich, I. Gruber, H. Heiss, C. A. Kiener, C. Krüger, J. U. Notheis, F. Rominger, G. Scherhag, M. Schultz, B. F. Straub, M. A. O. Volland, P. Hofmann, *New. J. Chem.* **2003**, *27*, 540–550.
[23] N. M. D. Brown, F. Davidson, R. McMullan, J. W. Wilson, *J. Organomet. Chem.* **1980**, *193*, 271–282.
[24] A. Sundararaman, F. Jäkle, *J. Organomet. Chem.* **2003**, *681*, 134–142.
[25] G. M. Sheldrick, *Acta Crystallogr., Sect. A* **2008**, *64*, 112–122.
[26] G. M. Sheldrick, *Acta Crystallogr., Sect. C* **2015**, *71*, 3–8.
[27] J.-D. Chai, M. Head-Gordon, *Phys. Chem. Chem. Phys.* **2008**, *10*, 6615–6620.
[28] Gaussian 09, Revision D.01, M. J. Frisch, G. W. Trucks, H. B. Schlegel, G. E. Scuseria, M. A. Robb, J. R. Cheeseman, G. Scalmani, V. Barone, B. Mennucci, G. A. Petersson, H. Nakatsuji, M. Caricato, X. Li, H. P. Hratchian, A. F. Izmaylov, J. Bloino, G. Zheng, J. L. Sonnenberg, M. Hada, M. Ehara, K. Toyota, R. Fukuda, J. Hasegawa, M. Ishida, T. Nakajima, Y. Honda, O. Kitao, H. Nakai, T. Vreven, J. A. Montgomery Jr., J. E. Peralta, F. Ogliaro, M. Bearpark, J. J. Heyd, E. Brothers, K. N. Kudin, V. N. Staroverov, T. Keith, R. Kobayashi, J. Normand, K. Raghavachari, A. Rendell, J. C. Burant, S. S. Iyengar, J. Tomasi, M. Cossi, N. Rega, J. M. Millam, M. Klene, J. E. Knox, J. B. Cross, V. Bakken, C. Adamo, J. Jaramillo, R. Gomperts, R. E. Stratmann, O. Yazyev, A. J. Austin, R. Cammi, C. Pomelli, J. W. Ochterski, R. L. Martin, K. Morokuma, V. G. Zakrzewski, G. A. Voth, P. Salvador, J. J. Dannenberg, S. Dapprich, A. D. Daniels, O. Farkas, J. B. Foresman, J. V. Ortiz, J. Cioslowski, D. J. Fox, Gaussian, Inc., Wallingford CT (USA), **2013**.
[29] a) R. Ditchfield, W. J. Hehre, J. A. Pople, *J. Chem. Phys.* **1971**, *54*, 724–728; b) W. J. Hehre, R. Ditchfield, J. A. Pople, *J. Chem. Phys.* **1972**, *56*, 2257–2261; c) P. C. Hariharan, J. A. Pople, *Theor. Chem. Acc.* **1973**, *28*, 213–222; d) P. C. Hariharan, J. A. Pople, *Mol. Phys.* **1974**, *27*, 209–214; e) M. S. Gordon, *Chem. Phys. Lett.* **1980**, *76*, 163–168; f) M. M. Francl, W. J. Pietro, W. J. Hehre, J. S. Binkley, D. J. DeFrees, J. A. Pople, M. S. Gordon, *J. Chem. Phys.* **1982**, *77*, 3654–3665; g) R. C. Binning Jr., L. A. Curtiss, *J. Comput. Chem.* **1990**, *11*, 1206–1216; h) J.-P. Blaudeau, M. P. McGrath, L. A. Curtiss, L. Radom, *J. Chem. Phys.* **1997**, *107*, 5016–5021; i) V. A. Rassolov, J. A. Pople, M. A. Ratner, T. L. Windus, *J. Chem. Phys.* **1998**, *109*, 1223–1229; j) V. A. Rassolov, M. A. Ratner, J. A. Pople, P. C. Redfern, L. A. Curtiss, *J. Comput. Chem.* **2001**, *22*, 976–984.
[30] For the polarization functions, see: M. J. Frisch, J. A. Pople, J. S. Binkley, *J. Chem. Phys.* **1984**, *80*, 3265–3269.

Received: November 28, 2019
Published Online: ■

Journal of Inorganic and General Chemistry
ZAAC
Zeitschrift für anorganische und allgemeine Chemie

*D. H. A. Boom, E. J. J. de Boed, E. Nicolas, M. Nieger, A. W. Ehlers, A. R. Jupp, J. C. Slootweg** **1–8**

Catalytic Dehydrogenation of Amine-Boranes using Geminal Phosphino-Boranes

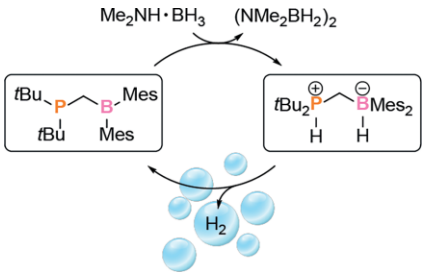

FLP Catalyzed Dehydrogenation

